Technical University of Denmark

DTU

Damping Behavior of Carbon Nanotube Reinforced Nanocomposites: Micromechanical Modeling and Experiments

Doagou Rad, Saeed; Jensen, Jakob Søndergaard; Islam, Aminul

Publication date:
2018

Document Version
Publisher's PDF, also known as Version of record

Link back to DTU Orbit

DTU Library
Technical Information Center of Denmark

DAMPING BEHAVIOR OF CARBON NANOTUBE REINFORCED NANOCOMPOSITES: MICROMECHANICAL MODELING AND EXPERIMENTS

S. Doagou-Rad[1,2], J. S. Jensen[1,2] and A. Islam[1,2]

[1] Department of Mechanical Engineering, Technical University of Denmark, Produktionstorvet, Building 427A, DK-2800 Kgs. Lyngby, Denmark,
Email: sadora@mek.dtu.dk, Web page: www.mek.dtu.dk
[2] Centre for Acoustic-Mechanical Microsystems (CAMM), Technical University of Denmark, Building 352, DK-2800 Kgs. Lyngby, Denmark
Email: sadora@mek.dtu.dk, Web page: http://www.camm.elektro.dtu.dk/

Keywords: Polymeric composites, Micromechanics, Damping, Modeling, Carbon nanotubes

Abstract
The damping characteristics of polymeric nanocomposites reinforced with carbon nanotubes is studied using micromechanical modeling and experiments. Two damage dissipation mechanisms namely interfacial and viscoelastic damping contribute to the damping properties of the polymeric nanocomposites. Incorporation of stiff fillers in the structure of the polymeric materials leads to a reduction of viscoelastic damping in the composites. However, inclusion of the nanotubes in the polymeric matrix also introduces a new dissipation mechanism along the interface with the polymeric phase. In order to study the dynamic behavior of the nanocomposites, normal and shear stress distributions along the nanotubes as the function of their orientation to the loading were achieved based on a shear-lag Cox model. Consequently, the slippage of the nanotube surrounded by polymeric phase as function of external loading and orientation of fibers was determined. Contribution of the viscoelastic damping to the nanocomposite behavior as the function of nanotube orientation and content was also studied. The total damping property of the nanocomposites represent the combined action of the two involved mechanisms. Nanocomposite specimens containing 0.5, 1.0, 3.0, 5.0, and 6.0 wt. % of the nanotubes were prepared. The damping and energy dissipation in the produced specimens were studied using dynamic mechanical experiments. Experimental results showed good agreement with the results abstained from the modeling.

1. Introduction

Damping properties are critical in many industrial applications. In fact, minimizing undesired noise and vibration in a variety of components such as machine elements, rotary-wing, sport and boating equipment, etc. is vital for their performance [1]. Different methods have been used to reduce vibration in the structures such as various types of viscoelastic polymeric damping tapes [2]. However, these applied conventional methods lead to various design and performance issues regarding reliability, safety, and maintenance. The increased weight and volume of the components particularly limits acquiring an optimal final functional product.
Replacing many industrial components by polymeric composites have been so intriguing due to the delivered advantages such as low-weights, high- processibility, flexibility to be shaped into complex structures, and corrosion resistance. Moreover, significant improvements in the mechanical properties of the polymeric composites such as stiffness, strength, and fracture behavior have already made them

indispensable for many advanced applications [3]. Therefore, the interests in improving their properties in different aspects are soaring sharply in industries such as automotive, defense, and aerospace. Application of polymeric composites in structural components inherently provided enhanced damping characteristics to the dynamic performance of the components. In fact, the damping properties of the polymers are some orders of magnitude higher than the traditionally used materials such as different metals. However, inclusion of traditional reinforcement agents such as glass fiber or carbon fiber in the polymeric matrixes results in the significant reduction of their potential damping properties. Therefore, the designers confronted with a trade-off between the static and dynamic performances.

The advent of nanofillers with their large interfacial areas and low densities provided a viable alternative to improve the performance of the composites multi-functionally. Studies showed that the inclusion of nanofillers such as carbon nanotubes (CNTs) could increase both loss modulus and stiffness of the polymeric composites [4]–[6]. In fact, the energy dissipation arising from the interfacial friction lead to the enhancement of damping properties, while preserving the structural integrity of the nanocomposites. This paper investigates the influence of carbon nanotubes inclusion into a polymeric matrix on the damping properties of the nanocomposites. The contributing damping mechanisms were modeled using micromechanics and finite element methods. The influence of the content and orientation of the nanofibers on the viscoelastic and interfacial damping properties of the nanocomposites was studied. Moreover, Polyamide 66 (PA 66) based composites reinforced with the different contents of the multi walled carbon nanotubes (MWCNTs) were produced, and their dynamic properties were studied in detail.

2. Experimental methods

The MWCNTs used in this study were catalytic chemical vapor deposition produced thin nanotubes (NC 7000 TM) by Nanocyl SA, Belgium. A Polyamide (PA 66) from ALBIS Plastic GmbH, Germany was used as the matrix. A conical counter rotating twin-screw extruder (HAAKE TM Rheomex CTW) was used to compound the nanocomposites with the different contents of 0.5, 1.0, 3.0, 5.0, and 6.0 wt. % of the nanotubes. Injection molding of the nanocomposite specimens was performed using a Ferromatik, Milacron, USA following the instructions of ISO 294-1. Dynamic mechanical characterization was also conducted on a MTS Acumen, USA [7].
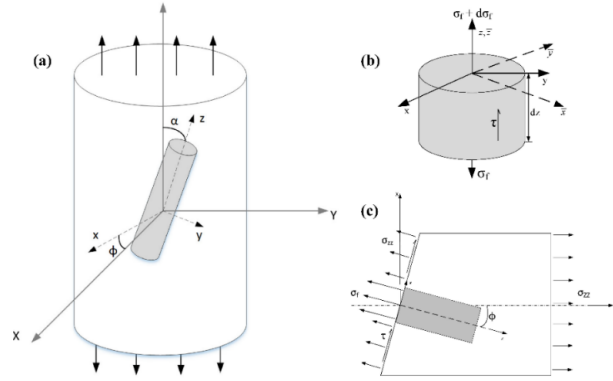
3. Modeling

Energy dissipation in carbon nanotube reinforced composites originates from two major mechanisms: Interfacial slippage and matrix viscoelastic damping. The two major phenomena were modeled through micromechanical models to investigate the influence of content and morphology on the damping behavior of the composites.

3.1. Interfacial Slippage

The interfacial characteristics in a nanocomposite is controlled by covalent and Van der Waals (VdW) attraction forces [4]. High strains lead to irreversible debonding within interfacial regions and the consequent failure. In this condition, all bonds in the interfacial areas are broken and the damage is permeant. However, the strain distribution arising from the dynamic loadings could initiate a partial slippage affecting just the VdW bonds in the interface between carbon nanotubes and the polymeric matrix. In other words, the strain levels and the shear forces are enough to overcome VdW interactions, while the covalent bonds are intact. Therefore, as the loads are removed, the slipped portions of the fibers retain their initial bonded positions. This sequential partial debonding and subsequent bonding contribute to the energy dissipation in a cycle of dynamic loading and damping of a mechanical structure. In order to study the influence of interfacial slippage contribution to the damping of a nanocomposite, a micromechanical modeling based on a Cox shear-lag model for discontinuous fiber reinforcements was

developed [8], [9]. Figure 1 illustrates the considered representative volume element of a nanocomposite reinforced with carbon nanotubes.

Figure 1. The representative volume element.

Some basic assumptions were also considered in the conducted modeling [10]:

i. Prior to the interfacial slippage, the bonding within the interfacial area is perfect;
ii. Along the nanofiber, the normal stress in the matrix is negligible compared to the normal stress in the fiber;
iii. The nanofibers are straight and do not buckle under loading;
iv. Nanofibers are perfectly distributed and dispersed in the matrix, and the stress fields do not interact.

From the equilibrium on an element of fibre with a length of dz (see Fig. 1(b)), the stresses are:

$$\int_0^{2\pi} \tau d\theta + \pi r_f \frac{d\sigma_f}{dz} = 0 \tag{1}$$

where σ_f is the normal stress in the nanotube along the fiber axis, independent of θ and r. This assumption, while the aspect ratio of the fillers are high and the reinforcement content is small becomes viable. Considering the same shear forces in the element, from Fig. 1(c) ($\gamma = \frac{\partial U_z}{\partial r} = \frac{\tau}{G_m}$):

$$U_m - U_f = \gamma_m (r_m - r_f) \tag{2}$$

where U_m and U_f are displacement of the composite and the nanotube along the fibre direction, respectively. γ_m is also engineering shear modulus in the matrix. r_m and r_f are radius values of volume element and nanofiller, respectively. Using the three-dimensional stress-strain relationships in combination with the first derivative of the Eq. 2 respect to z (i.e. $\frac{d\tau}{dz} = \frac{G_m}{r_m - r_f}(\varepsilon_m - \varepsilon_f)$) results to:

$$\frac{d\tau}{dz} = \frac{G_m}{r_m - r_f} \left[\sigma_{ZZ} \left(\frac{\cos^2 \alpha \cos^2 \phi}{E_m} - v_m \frac{\sin^2 \alpha \cos^2 \phi + \sin^2 \phi}{E_m} + v_f \frac{\sin^2 \alpha \cos^2 \phi + \sin^2 \phi}{E_f} \right) - \frac{\sigma_{zz,f}}{E_f} \right] \tag{3}$$

where τ is the shear stress acting on the interface and G_m is the shear modulus of the matrix. Since σ_m and σ_f are independent of z, $\frac{d\tau}{dz}$ is not a function of z. From Eq. 1 and 3 ($\frac{d^2\sigma_f}{dz^2} - A^2 \sigma_f = -B^2$):

$$\sigma_f = \frac{-B^2 / A^2}{\cosh \frac{Al_f}{2}} \cosh Az + \frac{B^2}{A^2} , \tag{4}$$

and

$$\tau = \frac{r_f}{2} \frac{B^2}{A} \frac{\sinh Az}{\cosh \frac{Al_f}{2}} + \sigma_{ZZ} * T(\alpha, \phi, \theta) , \tag{5}$$

where

$$\begin{cases} A^2 = \dfrac{2}{E_f r_f} \dfrac{G_m}{r_m - r_f} \\ B^2 = \dfrac{2}{r_f} \dfrac{G_m}{r_m - r_f} \left(\dfrac{\cos^2 \alpha \cos^2 \phi}{E_m} - v_m \dfrac{\sin^2 \alpha \cos^2 \phi + \sin^2 \phi}{E_m} + v_f \dfrac{\sin^2 \alpha \cos^2 \phi + \sin^2 \phi}{E_f} \right) \sigma_{ZZ} \end{cases}, \qquad (6)$$

and $T(\alpha, \phi, \theta)$ is attained from the boundary condition of the shear at the center of fiber. This term for two dimensional case will be $T = \sigma_{ZZ} \sin \theta \sin \alpha \cos \alpha$.

In order to study the achieved stress transfer relations, the analytical results were compared with the conducted finite element (FE) simulation results on a similar representative volume element. The FE simulations were conducted on a nanocomposites containing a single straight fiber using the commercial FE code ABAQUS implicit. A perfectly bonded interface between the polymer and fiber was implemented in the constructed models. The boundary conditions similar to dynamic mechanical experiments were imposed on the model where tangential displacements on the RVE outer surface are zero (Fig. 2(a)). Quadratic tetrahedral elements (C3D10) were also used to mesh the FE models. A python code was also developed to orient the fibers to the desired angles (see Fig. 2).
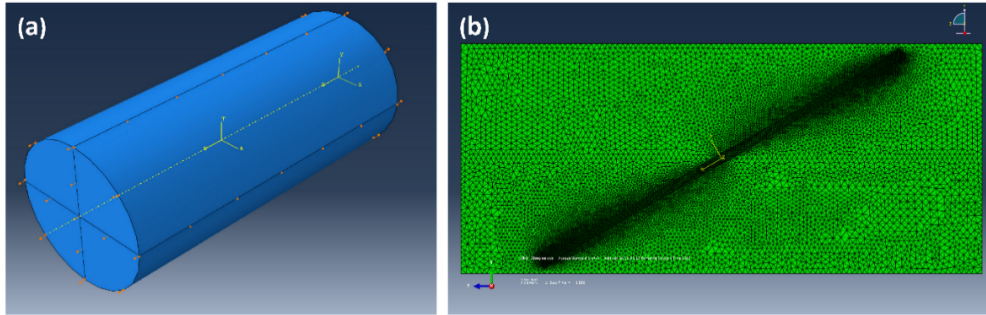
**Figure 2.** (a) Boundary conditions (b) the meshed model.

Figure 3 shows the obtained stress distributions from the performed FE simulations and micromechanical modeling. As it can be seen from the diagrams, both methods are leading to similar stress distributions along the included fiber. Acquiring a proper stress distribution was emphasized since the acquired stress fields in the interface essentially predict the initiation and extent of slippage. Therefore, the energy dissipation is determined by the attained stress fields. However, at the fiber tips, the FE modeling results diverged from the micromechanical modeling ones. This contrast in the results can be attributed to two differing parameters. First, in the analytical models, the stress transfer in the interfacial region is solely controlled by shear forces. Moreover, the major jump in the properties of the adjacent elements in the finite element model lead to some mathematical errors in the calculations.

Acquiring the interfacial stress fields allows calculation of energy dissipation and damping due to slippage in the interface. Interfacial slippage initiates when the shear stress in the interfacial region is higher than the critical shear stress (τ_c). Therefore, the shear stress at the slipped areas remains constant and equal to the critical shear stress. In other words, the slipped portion does not contribute to the load transfer following the slippage.

As slippage initiates, critical shear stress defines the stress at the tips of the fiber. Therefore, the critical input stress causing the initiation of the slippage process is attained as:

$$\sigma_{ZZ,c} = \dfrac{\tau_c}{\dfrac{r_f}{2} * A * S * \tanh \dfrac{Al_f}{2} + T(\alpha, \phi, \theta)}, \qquad (7)$$

where $\sigma_{ZZ,c}$ is the critical input stress that initiate slippage from the tips of included nanofibers.
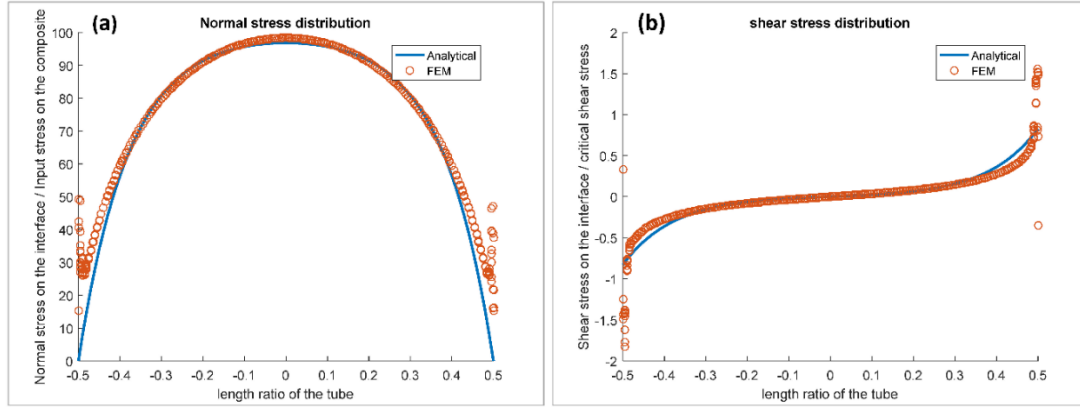
Figure 3. The (a) normal, and (b) shear distributions along the incorporated nanotube acquired from FE simulations and analytical modeling.

The length of slippage under the applied external loads higher than the critical input stress is achieved:

$$z_{slip} = l_f - \frac{2}{A}\sinh^{-1}\left(\frac{\tau_c * \cosh\frac{Al_f}{2}}{\frac{r_f}{2}*\frac{B^2}{A}} - \frac{\sigma_{ZZ}^2 * T(\alpha,\phi,\theta)*\cosh\frac{Al_f}{2}}{\frac{r_f}{2}*\frac{B^2}{A}}\right), \qquad (8)$$

where z_{slip} is slippage length along the fiber, and σ_{ZZ} is the applied stress on the nanocomposite. Moreover, τ_c is the critical shear stress determined by the interfacial properties and the bonding strength between the polymeric matrix and the nanofiller. A range of different values 2-15 MPa has been considered for this parameter in the literature [6]. Figure 4 illustrates the influence of critical shear stress on the stress distribution and slippage along the fiber. As it is expected, the higher critical shear stresses i.e. firm interface lead to lower slippage portion along the tubes. In other words, the composites are stiffer and higher input loads are required to trigger slippage damping contribution.

The loss factor is equal to ratio of dissipated energy to maximum strain energy per cycle. The maximum strain energy per cycle is achieved by:

$$U_0 = \frac{1}{2}\frac{V}{E_{Storage}}\sigma_\omega^2 = \frac{1}{2}*\left(\frac{A_f * l_f / 2}{vf_f}\right)*\frac{\sigma_\omega^2}{E_{Storage}}, \qquad (9)$$

where $E_{Storage}$ is the storage modulus of the composite in a cycle of loading:

$$E_{storage} = \frac{E_{storage}^{preslip} * \sigma_{ZZ,c} + \int_{\sigma_{ZZ,c}}^{\sigma_\omega} E_{Storage}^{postslip}(\sigma_{ZZ})d\sigma_{ZZ}}{\sigma_\omega}. \qquad (10)$$

The dissipated energy in a cycle is also attained by:

$$\delta U = \int_{\sigma_{ZZ,c}}^{\sigma_\omega}\int_0^{2\pi}\pi r_f \tau_{f,c} * z_{slip}^2(\sigma_{ZZ})*d\sigma_{ZZ}. \qquad (11)$$

Figure 5 presents the loss factor values arising from the interfacial slippage. As it can be noticed, while the damping remains nearly constant in lower nanofiller misalignments, it reduces significantly in orientations higher than 50 degrees. Moreover, the rate of enhancement in damping because of higher content of the nanotubes strictly depends on nanofiller orientation. For instance, while the fillers are misaligned 45 degrees, increasing the content of the nanotubes do not contribute to the interfacial damping effectively.
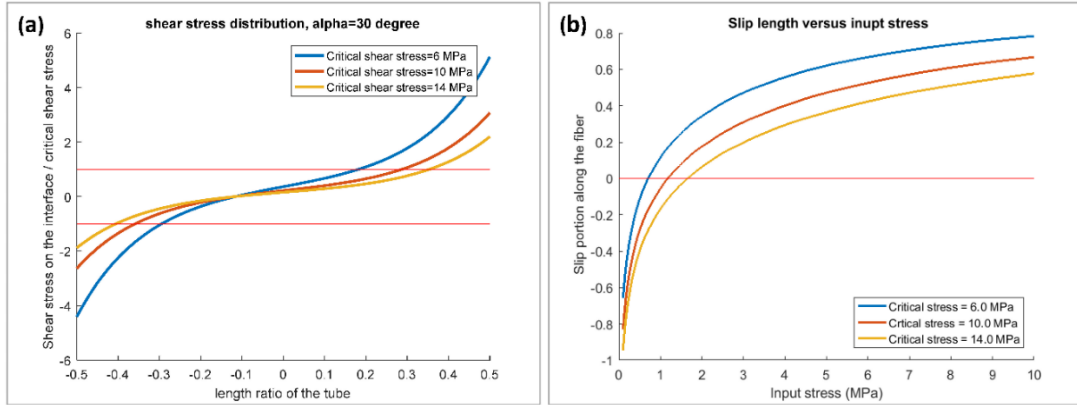
Figure 4. (a) Shear stress distribution along the fiber and (b) the extent of slippage as a function of interfacial strength and input stress.

3.2. Viscoelastic damping

Using the equivalent continuum model based on the Eshelby–Mori–Tanaka approach enables us to attain the homogenized stiffness matrix of the nanocomposites [11], [12]. The transversely isotropic stiffness matrix of the nanofillers and the isotropic elastic properties of the neat polymer is used as input in the micromechanical model to estimate the bulk elastic modulus of the nanocomposites including uniformly dispersed and straight carbon nanotubes. While the damping properties of the carbonic Nanoreinforcements are negligible, substituting the elastic modulus of the polymeric matrix by the complex modulus using elastic-viscoelastic correspondence principle leads to a real storage modulus and a complex loss modulus for the composites [13], [14]. Therefore, the damping properties arising from the viscoelastic properties of the composites can be attained as the ratio of achieved storage and loss moduli. The effective stiffness tensor $[C]$ of the two-phase nanocomposites can be estimated as [15]:

$$C_{complex} = C_m + c_r \left\langle \left(C_r - C_{m,complex} \right) A_r \right\rangle \left(c_m I + c_r \left\langle A_r \right\rangle \right)^{-1} \qquad (6)$$

where $C_{complex}$, $C_{m,complex}$ are nanocomposite and matrix complex stiffness tensors, respectively. In addition, C_r is the reinforcement stiffness tensor. c_m and c_r are also matrix and reinforcement volume fractions, and I is the identity tensor. A_r represents the dilute mechanical strain concentration tensor [16]. Acquiring the global stiffness matrix in the defined principal direction, global stiffness matrix of the nanocomposites comprising the carbon nanotubes that are oriented in other directions can also be obtained using transformation matrixes.
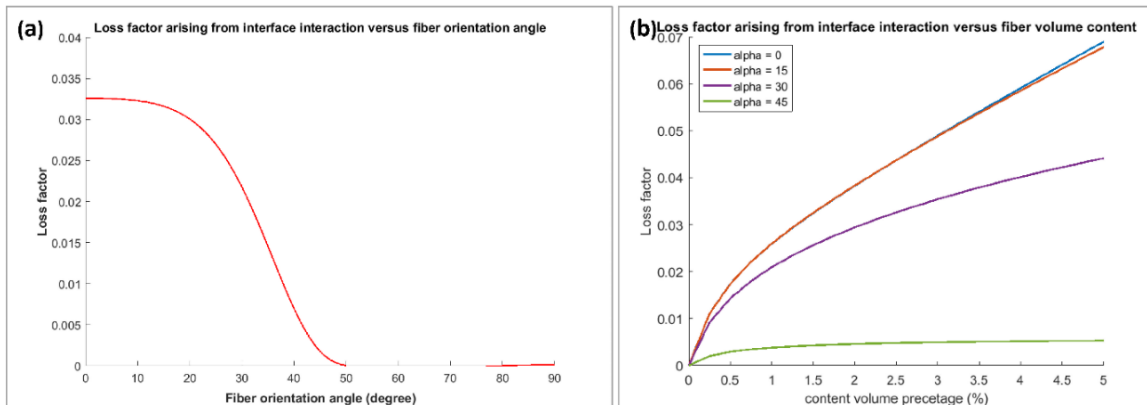

Figure 5. (a) Loss factors arising from the interfacial slippage as a function of nanotubes (a) orientations and (b) volume contents.

S. Doagou-Rad, J. S. Jensen, A. Islam

Figure 6 (a) presents the influence of fiber orientation on the viscoelastic damping of the composites. While the fillers are oriented in the direction of the applied loading axis, the composite is in its most stiff state, and it delivers the least viso-damping behavior. However, in contrast to interfacial damping, increase in the misalignment of fillers enhances the damping. In fact, in orientations higher than 60 degrees a similar viscoelastic behavior to the polymeric matrix could be expected. Figure 6 (b) illustrates the total damping behavior of the composites as the summation of the two counteracting phenomena of viscoelastic and interfacial damping. Results showed that in misalignment angles higher than 60 degrees a similar damping behavior as the polymeric matrix could be expected. However, an optimal nanofiller orientation is achieved where the inclusion of the nanofillers maximizes the damping of a nanocomposite plates. Such finding can be influential where the orientation of the nanofillers can be controlled by the methods such as hot-drawing or defining a proper gate position in microinjection molding.
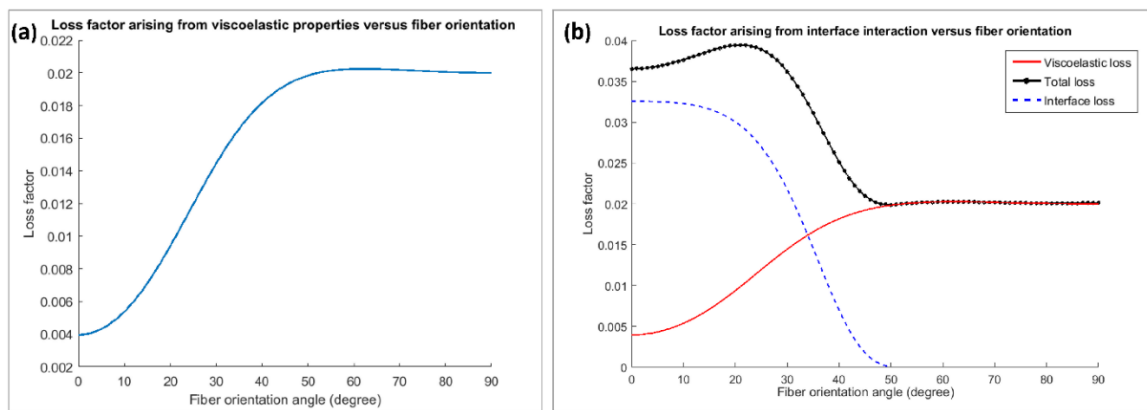
Figure 6. (a) Viscoelastic and (b) total damping of a nanocomposite plate as a function of fiber orientation.

Figure 7 illustrates the conducted dynamic-mechanical experimental results. As it can be noticed, increasing the content and input stress on the composites increased the energy dissipation in a cycle of loading. While loss moduli values of the neat polymer are nearly constant as the applied load increased, the nanocomposite loss moduli increased constantly. Fig. 7(b) shows the influence of the nanotube content on the interfacial slippage energy dissipation in the nanocomposites. As a random microstructure includes the produced nanocomposite morphologies, a similar trend to the modeling results can be observed. In fact, imposing 0.6 % strain (frequency = 1 Hz) on the composite systems increases interfacial loss factor up to 0.012 in nanocomposite containing 6.0 wt. % MWCNTs.
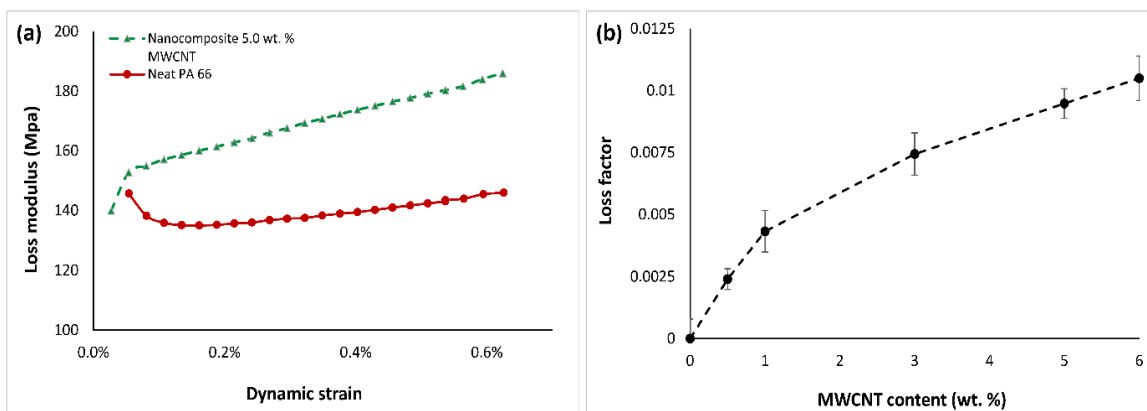
Figure 7. Influence of the applied (a) dynamic strain and (b) nanotube content on the loss properties of the composites.

4. Conclusions

The energy dissipation mechanisms in the nanocomposites reinforced with carbon nanotubes were studied. The damping properties arising from interfacial and viscoelastic properties were investigated and the influence of nanotube orientation and content on the dissipation mechanisms were studied. Results showed that the contribution of interfacial slippage to energy dissipation in the nanocomposite is significant. However, the acquired damping strictly depended on the fiber orientations. In fact, the influence of this mechanism decayed at misalignment angles more than 50 degrees. In addition, the influence of fiber orientation on the viscoelastic damping was studied and an optimal fiber orientation was attained for nanocomposite plates. Moreover, the produced nanocomposites were characterized experimentally. The results showed a multifunctional improvement in both stiffness and loss properties. The experimental results clearly confirmed the beneficial influence of nanotubes on the energy dissipation of the nanocomposites.

References

[1] A. Treviso, B. Van Genechten, D. Mundo, and M. Tournour. Damping in composite materials: Properties and models. *Composites Part B: Engineering*, 78:144–152, 2015.

[2] J. B. Kosamata and S. L. Liguore. Review of methods for analyzing constrained layer damping structures. *J. Aerospace Eng*, 6:268–283, 1993.

[3] B. Glaz, J. Riddick, E. Habtour, and H. Kang. Interfacial strain energy dissipation in hybrid nanocomposite beams under axial strain fields. *AIAA Journal*, 53:1544–1554, 2015.

[4] F. Gardea, B. Glaz, J. Riddick, D. C. Lagoudas, and M. Naraghi. Energy dissipation due to interfacial slip in nanocomposites reinforced with aligned carbon nanotubes. *ACS applied materials & interfaces*, 7:9725–9735, 2015.

[5] J. Suhr and N. A. Koratkar, "Energy dissipation in carbon nanotube composites: a review. *Journal of Materials Science*, 43:4370–4382, 2008.

[6] T. Ogasawara, T. Tsuda, and N. Takeda, Stress–strain behavior of multi-walled carbon nanotube/PEEK composites. *Composites Science and Technology*, 71:73–78, 2011.

[7] S. Doagou-Rad, A. Islam, and J. Søndergaard Jensen. Correlation of mechanical and electrical properties with processing variables in MWCNT reinforced thermoplastic nanocomposites. *Journal of Composite Materials*, p. 2199831876839, 2018.

[8] H. L. Cox, The elasticity and strength of paper and other fibrous materials. *British Journal of Applied Physics*, 3:72–79, 1952.

[9] A. Kelly. Interface Effects and the Work of Fracture of a Fibrous Composite. *Proceedings of the Royal Society of London A: Mathematical, Physical and Engineering Sciences*, 319:95–116, 1970.

[10] C. T. Chon and C. T. Sun. Stress distributions along a short fibre in fibre reinforced plastics. *Journal of Materials Science*, 15:931–938, 1980.

[11] T. Mori and K. Tanaka. Average stress in matrix and average elastic energy of materials with misfitting inclusions. Acta Metall., 21:571–574, 1973.

[12] J. D. Eshelby, The determination of the elastic field of an ellipsoidal inclusion, and related problems. *Proceedings of the Royal Society of London A: Mathematical, Physical and Engineering Sciences*, 241:376–396, 1957.

[13] R. F. Gibson, S. K. Chaturvedi, and C. T. Sun. Complex moduli of aligned discontinuous fibre-reinforced polymer composites. *Journal of Materials Science*, 17:3499–3509, 1982.

[14] C. T. Sun, S. K. Chaturvedi, and R. F. Gibson. Internal damping of short-fiber reinforced polymer matrix composites. *Computers and structures*, 20:391–400, 1985.

[15] Y. Benveniste. A new approach to the application of Mori-Tanaka's theory in composite materials. *Mechanics of materials*, 6:147–157, 1987.

[16] T. Mura, *Micromechanics of defects in solids*. Martinus Nijhoff Publishers, 1982.